

Image Quality Comparison of Filter Placement Effect on the LWIR Camera of LAPAN A4 Satellite

Rommy Hartono¹, Dede Ardianto¹, A Hadi Syafrudin¹

¹Research Center for Satellite Technology,
National Research and Innovation Agency (BRIN), Indonesia
e-mail: romm001@brin.go.id

Received: 19-06-2023. Accepted: 20-03-2024. Published: 31-12-2024

Abstract

The LAPAN A4 LWIR camera has already been installed with a bandpass filter, generating a spectral response whose value is near the spectral response of TIRS bands 10 and 11 of LANDSAT 8. Due to the small size of the mechanical part of the LWIR bandpass filter, which has a diameter of 32.5mm, a problem arises when installing the LWIR filter. The filter can be placed in four different positions inside the LWIR camera, and these four positions are also viable for capturing images. This paper aims to compare images generated from four possible filter placements on the LWIR camera using the LAPAN LWIR filter to obtain the best image quality from the LAPAN LWIR camera. To achieve optimal results from these four possible placements, statistical analyses such as standard deviation, SNR calculation, dynamic range, and spatial response area using a moving average filter are employed to assess image quality. Based on the tests and the analysis of signal-to-noise ratio and dynamic range, filter placements behind the zoom lens and in front of the focus lens are nearly identical and superior to those in front of the zoom lens and behind the focus lens. Conversely, the analysis of spatial response area using a moving average filter shows that the filter in front of the zoom and focus lens is superior to that behind the zoom lens. Therefore, the recommendation is to place the filter in front of the zoom and focus lens for the final assembly.

Keywords: *filter, lens, image, placement, statistic analysis, LAPAN LWIR.*

1. Introduction

The primary mission of the LAPAN-A4 satellite is earth observation using a medium-resolution imager (MRI) from Surrey Satellite Technology Ltd (SSTL), which has been considered for the LAPAN-A4 mission. This payload utilizes the CANBus interface for communication (Hartono et al., 2018). The next payload is the Experimental LAPAN Line Imager Space Application Camera (ELLISA), which has two types of resolutions: medium and high (Saifudin et al., 2018). Other payloads include an experimental Short-Wave Infrared (SWIR) camera (Salaswati et al., 2020) and a Long Wave Infrared (LWIR) camera called a microbolometer. Two microbolometer cameras are on the LAPAN-A4 satellite: LAPAN LWIR and LWIR BPPT.

The LWIR camera on the LAPAN-A4 satellite has the following specifications: a spectral band of 8-14 μ m, an array type a-Si microbolometer, a pixel size of 640 (W) x 480 (H), a pixel pitch of 17 μ m, a frame rate of 50 Hz, no cooling, a 16-bit A/D conversion resolution, and an interface using base camera link (CL) (Xenics Infrared Solution, 2016). Specifically, a bandpass filter has already been installed for the LAPAN LWIR camera (Hartono et al., 2019). This bandpass filter can generate a spectral response output with a cut-on wavelength at 10400 nm and a cut-off wavelength at 12500 nm. The bandpass filter also has a central wavelength (CWL) at 11450 nm, and the bandwidth is 2100 nm. The spectral response from the LWIR filter is close to the spectral response from TIRS bands 10 and 11 of LANDSAT 8, where band 10 has a spectral response of 10600 nm – 11900 nm, and band 11 has a spectral response of 11500 nm – 12510 nm (Reuter et al., 2015) (Barsi et al., 2014).

From the previous paper (R. Hartono et al., 2019), the filter will be installed between the LWIR camera and the lens with a discrepancy of 150 mm after obtaining the spectral response. The shape of the bandpass filter of LAPAN LWIR is a circle with a diameter of approximately 32.5 mm and a thickness of 1 – 2 mm. However, due to the mechanical size issue of the bandpass filter being too small, a new problem arises: the filter installation can be placed in four different positions on the LAPAN LWIR camera.

To obtain the best image from various positions of a filter on LAPAN LWIR, several statistical analyses, including standard deviation, signal-to-noise ratio (SNR) calculation, dynamic range, and spatial response area using a moving average filter, are required. The objective of this paper is to compare images from four potential filter placements. Subsequently, image processing analyses will be conducted individually to determine the optimal filter placement on the LAPAN LWIR camera. The results will serve as a reference for the preprocessing of radiometry calibration on the LAPAN LWIR camera.

This paper is organized as follows: the first section is the introduction, and the second section covers the methodology, including the general theory about the statistical analysis of image quality used in this research. The following section details the implementation of possible filter placements on the LAPAN LWIR camera, divided into two-step parameter characterization of LAPAN LWIR and the test results. This is followed by statistical analysis and discussion. The final section includes the conclusion of this research and suggestions for future work.

2. Methodology

As described at the beginning, the problem arises due to the small dimensions of the LWIR filter, allowing it to be positioned or placed in various positions on the LAPAN LWIR lenses. This paper aims to address and resolve this issue. The method used in this paper is comparing images from four possible placements of the LAPAN LWIR filter on without using the LAPAN LWIR (original) filter. All the images will be analyzed to obtain the best result. The four possible placements of filter LAPAN LWIR are: (1) The filter is placed in front of the zoom lens (between the primary lens and the zoom lens), (2) The filter is placed behind the zoom lens (between zoom lens and center lens), (3) The filter is placed in front of the focus lens (between the center lens and focus lens), and last (4) The filter is placed behind the focus lens (between focus lens and sensor camera).

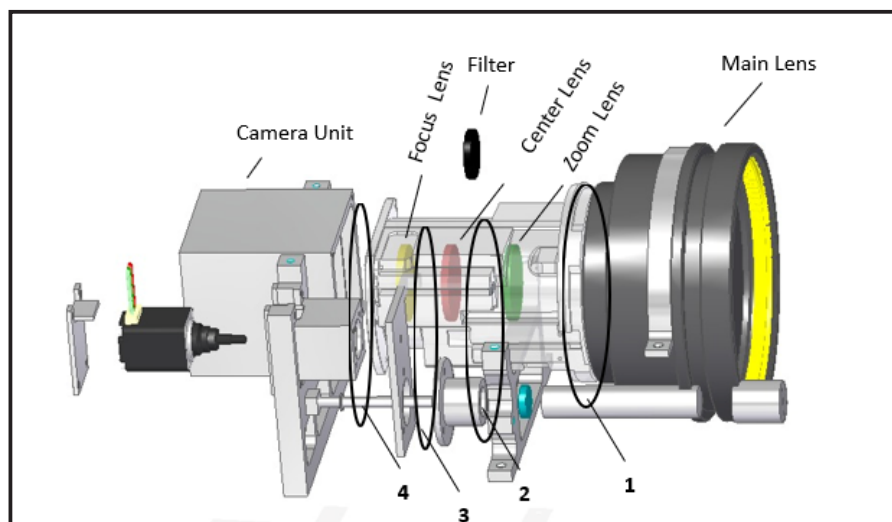


Figure 2-1: Visualization of the Filter Assembly on the Camera.

The images captured and analyzed maintain identical positions, objects, and camera parameter characteristics as those captured without using the LAPAN LWIR filter. Following the acquisition of images for each filter placement, the subsequent step involves analyzing all photos by calculating the signal-to-noise ratio, standard deviation, dynamic range, and moving average filter. The final step is to provide recommended techniques based on the conducted analysis. The overall methodology employed in this research is outlined in Figure 2-1.

The quality of an image is a critical aspect of image processing applications. Firstly, it serves the purpose of dynamically monitoring and adjusting image quality. Secondly, it aids in optimizing algorithms and parameter settings within image processing systems. Lastly, it facilitates the tracking of processing systems and algorithms (Zhang et al., 2016; Yang & Ming, 2016).

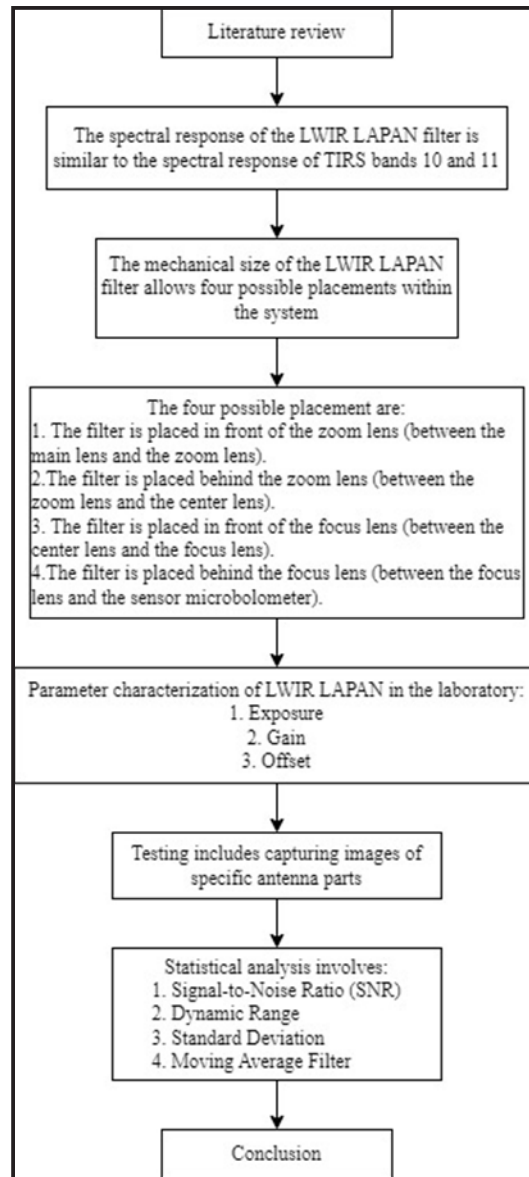


Figure 2-2: Flow Chart of the Methodology.

In comparing the results of images produced from possible placements of the filter, the methods used are the calculation of SNR, dynamic range, standard deviation, and the maximum, minimum, and average values of the digital number produced by a picture that has been tested before and moving average filter. This paper focuses on the statistical measurements of image quality to get the best possible filter placement and image. The measurements mentioned are SNR, standard deviation, dynamic range, and moving average filter.

2.1. Signal to Noise Ratio

The signal-to-noise ratio is the ratio between the average signal value and the signal value's standard deviation (Fu et al., 2016; Vlachos & Dermatas, 2012). A higher SNR value indicates better image quality and a lower SNR indicates a specific region of the image weakness relative to background noise (Mustafa & Yazid, 2016; Mustafa, Yazid, & Yaacob, 2015). $I(x,y)$ represents the input image, and $StdDev[I(x,y)]$ is the standard deviation of the image. The equation is as follows:

$$SNR = 0 \log_0 \frac{Mean[I(x, y)]}{StdDev[I(x, y)]} \quad (2-1)$$

2.2. Standard Deviation

One of the methods for image enhancement on statistical measurement is scaled by the standard deviation. The standard deviation expression represents the image's contrast (Sergyan, 2008). If the standard deviation is high, then it shows the high contrast of the image, but if the low standard deviation indicates low contrast in the image. The equation of standard deviation is as follows:

$$S_{(x,y)} = \frac{1}{w} \left[\sum_{x-w}^{x+w} \sum_{y-w}^{y+w} [F(m,n) - M(m,n)]^2 \right]^{1/2} \quad (2-2)$$

where $F(x, y)$ and $S(x, y)$ indicate the original pixel value and standard deviation, respectively, while $M(m, n)$ indicates the mean value of the image part (Cano-Garcia et al., 2012).

2.3. Dynamic Range

The dynamic range (DR) from an image indicates the ability of the imager to resolve detail in dark areas as well as detail in bright areas in the same image, and it shows the largest detectable signal versus the smallest detectable signal (Vallat-Evrard et al., 2019). The equation is defined as:

$$DR = 0 \log \frac{DN_{Saturation}}{DN_{Noise}} \quad (2-3)$$

where DR is dynamic range, $DN_{Saturation}$ is digital number saturation signal of the sensor, and DN_{Noise} is digital number noise in dark

2.4. Moving Average Filter

The moving average filter operates with an average number of points from the input signals to generate each point on the output signal (Smith, 1999). Equation 2-4 shows the theory of moving average filter.

$$y[n] = \frac{1}{M} \sum_{k=0}^{M-1} x[n-k] \quad (2-4)$$

where $x[]$ is the input signal, $y[]$ is the output signal, and M indicates the number of points used in the moving average filter. This equation only uses points on one side of the output sample for calculation. For example, a seven-point moving average filter is used in this research. Equation 2-5 shows a sample of input and calculates the average in this paper.

$$y[n] = \frac{1}{7} \left(x[n] + x[n-1] + x[n-2] + x[n-3] + x[n-4] + x[n-5] + x[n-6] \right) \quad (2-5)$$

After using a moving average filter, the next step is adding an offset into the moving average filter analysis. The offset value can be a positive or negative number. Offset is served to raise the value of the digital number of the four possible filter placements calculated with the moving average filter over the digital number without using a filter.

3. Implementation of Filter Placement

3.1 Parameter Characterization of LAPAN LWIR

Parameter characterization is a prerequisite for producing high-quality scientific data and high-level downstream products. Stable image quality is required during radiometric calibration to extract signal characteristics from the data obtained by the sensor (Teillet et

al., 2001). Satellite images have their own calibration and correlation with calibration on the ground before launch or pre-flight. Possible different factors are vacuum and temperature, which cannot be simulated on the ground (Syafudin et al., 2018). Characterization is one of the crucial things to do because it can be a reference for orbit calibration and estimation errors caused and studied for future calibration projects. This characterization needs to be conducted so the image of the LAPAN LWIR camera can be known in conditions with or without illumination.

Before conducting tests on the filter placement of the LAPAN LWIR camera, the primary parameters that have already been characterized include exposure, gain, and offset of the LAPAN LWIR camera with the filter. The test involved determining the digital number closest to the average Analog-to-Digital Converter (ADC) value of the LWIR camera. The approach for the characterization of the LWIR camera involved (1) the characterization of a dark camera by closing the shutter and (2) the characterization of camera parameters (exposure, gain, and offset) to digital numbers (DN) on the camera. The parameter characterization of the LWIR camera, featuring the optimal setting of digital numbers (DN) when using a filter, is presented in Table 3-1.

Table 3-1: LAPAN LWIR Characterization.

Parameter LWIR Camera With Filter	Range Value	Best Value	Unit
Exposure	0–80	40	us
Gain	0–255	40	
Offset	-99 until 100	-10	

3.2 Test Result

The tests were done in the Assembly, Integration, and Testing (AIT) laboratory of the Satellite Technology Center, and the image retrieval was done by comparing the result of four possible placements of the LAPAN LWIR filter, taking parts of the antenna image, such as horn and pedestal.

From the test of possible placement for LAPAN LWIR filter for horn antenna, we can compute signal-to-noise ratio value and dynamic range using equations 2-1, 2-2, and 2-3. The values of SNR for the case of without filter / original and with filter for 1st, 2nd, 3rd, and 4th placements for horn antenna object are as follows:

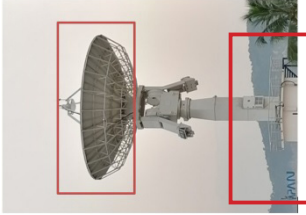

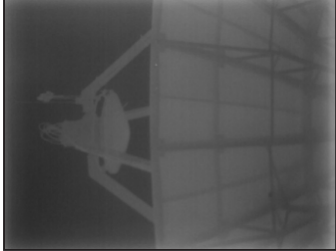



Table 3-2: SNR Comparison for Horn Antenna.

SNR				
Without Filter	Placement			
	1	2	3	4
2.055	5.026	8.340	7.717	11.316

Table 3-3: Dynamic Range Comparison for Horn Antenna.

Dynamic Range				
Without Filter	Placement			
	1	2	3	4
46992	28720	21648	22192	16976

Table 3-4: Horn Antenna Object as the First Test.

 <p>Target test</p>		
 <p>Without Filter/ Original Max = 50080 Min = 3088 Mean = 25315 STD Dev = 12316</p>	 <p>Front of the zoom lens (Placement 1) Max = 39376 Min = 10656 Mean = 21344 STD Dev = 4247</p>	 <p>Behind the zoom lens (Placement 2) Max = 38608 Min = 16960 Mean = 25469 STD Dev = 3054</p>
 <p>In front of the focus lens (Placement 3) Max = 38736 Min = 16544 Mean = 25257 STD Dev = 3273</p>	 <p>Behind the focus lens (Placement 4) Max = 39376 Min = 22400 Mean = 31877 STD Dev = 2817</p>	<p>Every camera has the same setting parameters:</p> <p>Exposure = 40 Offset = -10 Gain = 40</p>

On the other hand, the signal-to-noise ratio values for the case without filter (original) and with filter 1st, 2nd, 3rd, and 4th placements for pedestal antenna object are as follows:

Table 3-5: SNR Comparison for Pedestal Antenna.

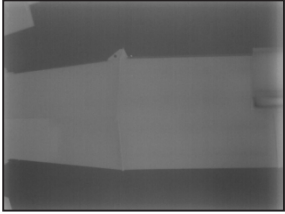
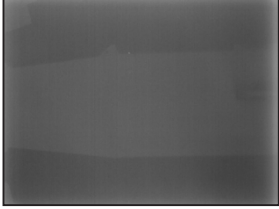
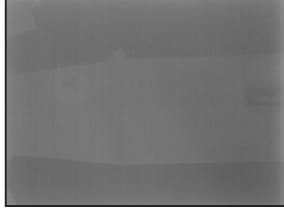
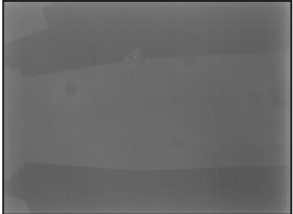

SNR				
Without Filter	Placement			
	1	2	3	4
12.745	10.663	21.625	18.319	22.714

Table 3-6: DR Comparison for Pedestal Antenna.

Dynamic Range				
Without Filter	Placement			
	1	2	3	4
25312	21936	14464	16512	12336

Based on the tests carried out and the analysis of the results of the signal-to-noise ratio (SNR) and dynamic range, the higher the SNR and the dynamic range values, the better the resulting image will also be. A larger dynamic range and higher SNR are preferable. Therefore, the hypothesis suggests that filter placements in the 2nd and 3rd positions are almost identical and better than those in the 1st and 4th positions. However, the results of SNR and DR were not used as conclusions because many factors influence the placement of the LAPAN LWIR filter.

Table 3-6: Pedestal Antenna Object as the Second Test.

 <p>Without Filter/ Original Max = 40672 Min = 15360 Mean = 25733 STD Dev = 2019</p>	 <p>Front of the zoom lens (Placement 1) Max = 38320 Min = 16384 Mean = 23639 STD Dev = 2217</p>	 <p>Behind the zoom lens (Placement 2) Max = 37824 Min = 23360 Mean = 29496 STD Dev = 1364</p>
 <p>In front of the focus lens (Placement 3) Max = 37776 Min = 21264 Mean = 27497 STD Dev = 1501</p>	 <p>Behind the focus lens (Placement 4) Max = 38112 Min = 25776 Mean = 32526 STD Dev = 1432</p>	<p>Every camera has the same setting parameters</p> <p>Exposure = 40 Offset = -10 Gain = 40</p>

4. Statistical Analysis and Discussion

After completing the characterization and testing of the LAPAN LWIR camera and calculating statistical analysis values such as SNR, STD Dev, and dynamic range, the final analysis involves the moving average filter. Before beginning this process, the first step is to measure the spatial response by comparing the area ratios of the curve with and without the use of a filter. The calculation involves a simple comparison of digital number values with and without a filter. The bandpass filter for the LAPAN LWIR camera was designed to generate the expected spectral response output. For details, please refer to Figure 4-1, which illustrates the spectral comparison of input and output wavelengths.

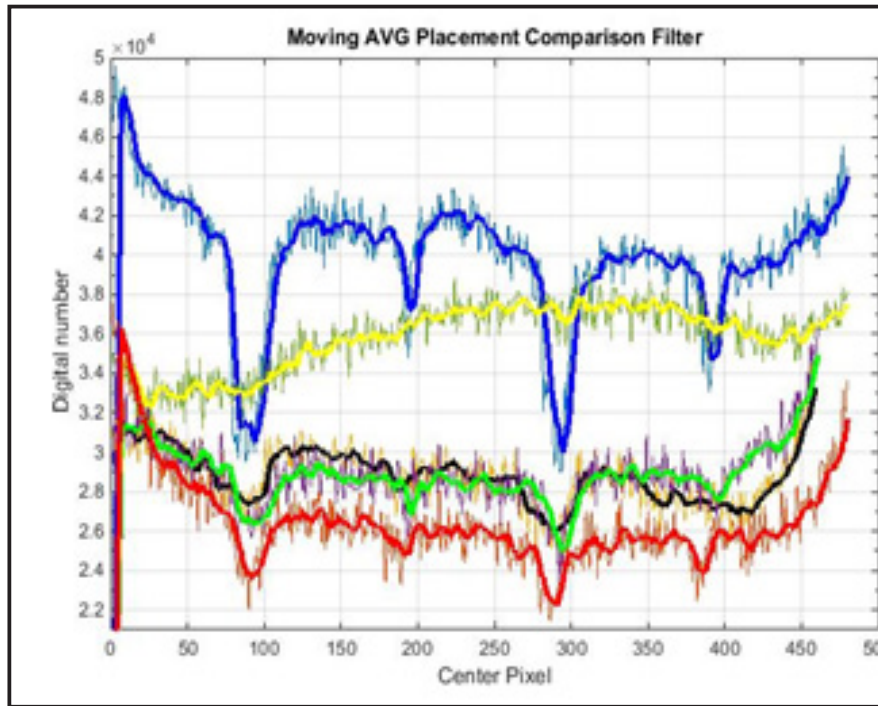


Figure 4-1: LAPAN LWIR Filter Response.

The designed bandpass filter demonstrates an average transmission of 76.94%, with a maximum transmission reaching 80.21%. The transmission value must exceed 75% to transmit power (Yang & Ming, 2016) effectively. The transmission value is expressed as a percentage, representing the proportion of power received by the detector relative to the total available power. According to the design results (Hartono et al., 2019), the spectral response value without a filter is from 8000 nm to 14000 nm, resulting in a bandwidth of 6000 nm. Meanwhile, the filter's spectral response value is 10420 nm to 12480 nm, reducing the bandwidth to 1648 nm. This leads to a spatial response ratio area curve between with and without filter (original) of 27.467%. The comparison value serves as a reference for the approach when using a filter.

To get an analysis of the measurement of spatial response area of the curve, the calculation uses the moving average filter method. The moving average filter calculation according to Equation 2-5, was easy to realized. By including the argument as the numerator and denominator as coefficients, they were used for rational transfer function specified as a vector. Figure 4-2 below is an implementation of the moving average filter of the horn antenna in which the digital number of the image produced from four possible placements of the LAPAN LWIR filter is very low. Hence, comparing the spatial response area of the curve between images with and without filter (original) was challenging. For that reason, to determine the comparative analysis of the spatial response area of the curve, adding a positive offset value is required in a low-value digital number or the image with filter so that the digital number can be close to the digital number of images without a filter (original).

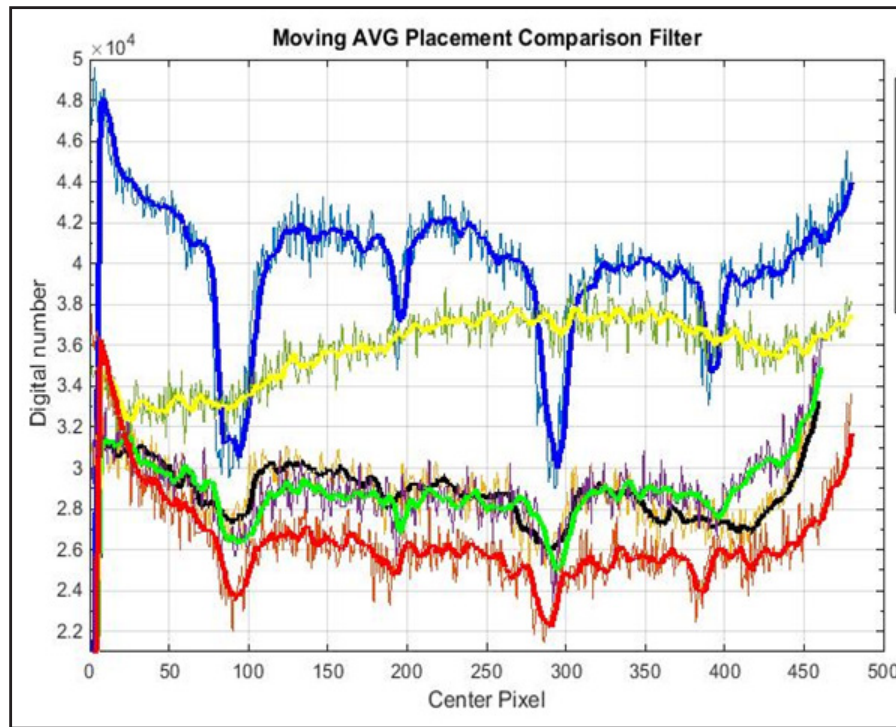


Figure 4-2: Moving Average Filter for Horn Antenna Object.

Figure 4-2 can be described as follows: the blue curve represents the response without a filter (original), the red curve represents the response with a filter placed in front of the zoom lens (between the main lens and the zoom lens), the black curve represents the response with a filter placed behind the zoom lens (between the zoom lens and the center lens), the green curve represents the response with a filter placed in front of the focus lens (between the center lens and the focus lens), and the yellow curve represents the response with a filter placed behind the focus lens (between the zoom lens and the LAPAN LWIR sensor).

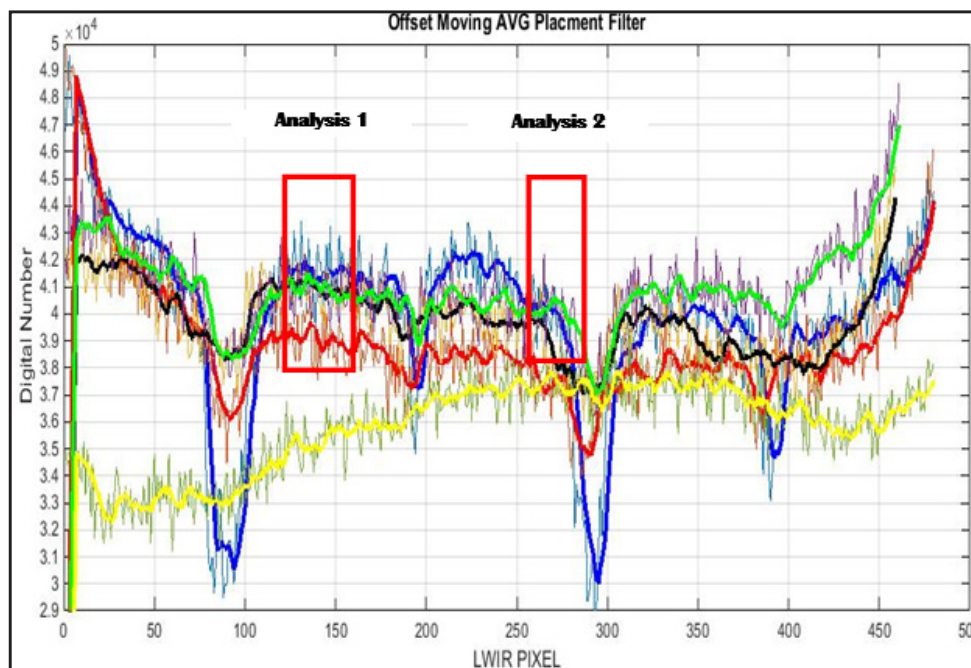


Figure 4-3: Moving Average for Horn Antenna Object with Offset Parameter.

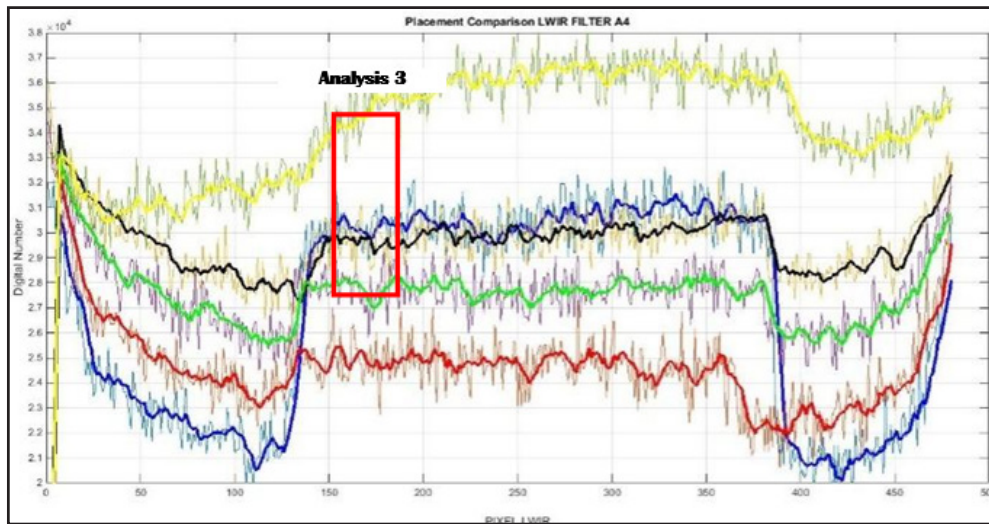


Figure 4-4: Moving Average for Pedestal Antenna Object with Offset Parameter.

Figures 4-3 and 4-4 depict the implementation of adding a digital number offset to images using a filter. Once the digital numbers align with the values of the images without a filter (original), the curve's spatial response area can be compared. In this paper, three spatial response comparisons were performed. The sample analysis in this project uses one axis for sampling each pixel, minimizing the vignetting effect and different pixel characteristics. The first and second analyses were done in Figure 4-2 (horn antenna) with spatial response analysis at pixels 100 and 300. The third analysis done in Figure 4-3 (pedestal antenna) is on pixel 100.

Based on Figure 4-2, analysis was done by comparing the initial value of the digital number when going down with the digital number when rising from the bottom of the wave. In the case of Figure 4-3, the analysis was done by comparing the initial value of the digital number when rising with the digital number when going down from the top of the wave.

We can get the three conditional analyses from the LAPAN LWIR filter placement test based on spatial response comparison calculation. The analysis results can be seen in Table 4-1 below.

Table 4-1: Resume of Placement Test of LWIR Filter.

1 st analysis condition	Antenna horn object				
	First DN	Last DN	Bandwidth	Comparison ratio (%)	Reference Ratio (%)
Without Filter/original	4100	3100	1000	-	-
Front of the zoom lens (1)	3900	3650	250	25%	27.4%
Behind the zoom lens (2)	4000	3850	150	15%	
In front of the focus lens (3)	4100	3850	250	25%	
Behind the focus lens (4)	Cannot be processed		-	-	
2 nd analysis condition	Antenna horn object				
	First DN	Last DN	Bandwidth	Comparison ratio (%)	Reference Ratio (%)
Without Filter/original	4000	3000	1000	-	-
Front of the zoom lens (1)	3750	3500	250	25%	27.4%
Behind the zoom lens (2)	3950	3740	200	20%	
In front of the focus lens (3)	4050	3700	350	35%	
Behind the focus lens (4)	Cannot be processed		-	-	

3 rd analysis condition	Antenna horn object				
	First DN	Last DN	Bandwidth	Comparison ratio (%)	Reference Ratio (%)
Without Filter/original	3100	2100	1000	-	27.4%
Front of the zoom lens (1)	2500	2200	300	30%	
Behind the zoom lens (2)	3050	2850	200	20%	
In front of the focus lens (3)	2800	2600	200	20%	
Behind the focus lens (4)	Cannot be processed		-	-	

Meanwhile, the results of the moving average analysis can be summarized as follows.

Table 4-2: Moving Average Analysis.

Filter Location	In front of the zoom lens (1)	Behind the zoom lens (2)	In front of the focus lens (3)
Analysis 1	250	150	250
Analysis 2	250	210	350
Analysis 3	300	200	200
Average	266.67	186.67	266.67

The first paragraph explained that the bandwidth value of the spatial response ratio area curve between the filter and the original (without filter) is 27.467%. Therefore, based on the summaries provided in Table 4.1 and Table 4.2 for the LWIR filter placement test, it is evident that a larger spatial response fidelity is preferable. Consequently, filter placements in the 1st and 3rd positions are nearly identical and superior to those in the 2nd and 4th positions. This conclusion is drawn from their comparison ratio approaching the designated reference value of 27.4%.

Based on testing and analysis that has been done in this paper, from the analysis of the SNR, dynamic range, and spatial response calculation using moving average filter, the recommendation of the best placement of LAPAN LWIR filter is 1st position (the filter is placed in front of the zoom lens which is between the primary lens and zoom lens) and 3rd position (the filter is placed in front of the focus lens which is between the center lens and focus lens). The analysis of multiple image recordings also influences the recommendation for the optimal placement of the LAPAN LWIR filter. The placement of filters in the 1st and 3rd positions requires further discussion with the LAPAN-A4 structural department. This is necessary to address mounting or framing considerations to ensure the proper installation of the filter.

5. Conclusions

The problem arises due to the small dimensions of an LWIR filter, allowing it to be placed in several positions on LAPAN LWIR lenses. There are four possible placements for the LAPAN LWIR filter. Based on the implemented placement of the LAPAN LWIR filter and the discussion results in chapters 3 and 4, the conclusion is that the 1st and 3rd placements are optimal from the perspectives of SNR, dynamic range, and spatial response area of the curve using the moving average filter method, influenced by multiple image recordings conducted.

Acknowledgments

The authors would like to thank Dr.-Ing. Wahyudi Hasbi, S.Si., M.Kom., as the head of the Research Center for Satellite Technology, National Research and Innovation Agency, for his support so that this research can be well completed.

Contributorship Statement

Rommy Hartono, Dede Ardianto, and A Hadi Syafrudin have the same role as the main contributors in this research, who are responsible for the research design process and testing procedures, as well as processing and analysis of the data.

References

- Hartono, R., Syafrudin, A. H., Hasbi, W., & Yatim, R. (2018). Implementation Of CAN Bus Communication To UART In LAPAN-A4 Satellite. In *IEEE International Conference on Aerospace Electronics and Remote Sensing Technology (ICARES)* (pp. 1-7). Bali: IEEE. doi:10.1109/ICARES.2018.8547149
- Saifudin, M. A., Karim, A., & Mujtahid. (2018). LAPAN-A4 Concept and Design for Earth Observation and Maritime Monitoring Missions. In *IEEE International Conference on Aerospace Electronics and Remote Sensing Technology (ICARES)* (pp. 1-5). Bali: IEEE. doi: 10.1109/ICARES.2018.8547143.
- Salaswati, S., Hartono, R., Ardianto, D., & Syafrudin, A. H. (2020). Radiometric characterization for short wave infrared (SWIR) camera of LAPAN-A4 satellite. *AIP Conference Proceedings*, 2226(1), 030009. <https://doi.org/10.1063/5.0003785>
- Xenics Infrared Solution. (2016). *User Manual Gobi-640-17μm GigE/CL/CXP Camera and Gobi-384-25μm GigE/CL Camera* (Doc: ENG-2012-UMN007-R013 : 007). Belgium.
- Hartono, R., Ardianto, D., Salaswati, S., Yatim, R., & Syafrudin, A. H. (2019). Design Requirement of LWIR Optical Filter for LAPAN-A4 Satellite. In *2019 IEEE International Conference on Aerospace Electronics and Remote Sensing Technology (ICARES)* (pp. 1-7). doi: 10.1109/ICARES.2019.8914354.
- Reuter, D.C., Richardson, C.M., Pellerano, F.A., Irons, J.R., Allen, R.G., Anderson, M., Jhabvala, M.D., Lunsford, A.W., Montanaro, M., Smith, R.L., Tesfaye, Z., & Thome, K.J. (2015). The Thermal Infrared Sensor (TIRS) on Landsat 8: Design Overview and Pre-Launch Characterization. *Remote Sens.*, 7, 1135-1153. <https://doi.org/10.3390/rs70101135>
- Barsi, J.A., Lee, K., Markham, B.L., Kvaran, G., & Pedelty, J.A. (2014). The spectral response of the Landsat-8 Operational Land Imager. *Remote Sens.*, 6, 10232–10251.
- Zhang, Y., Wu, J., Xie, X., Li, L., & Shi, G. (2016). Blind image quality assessment with improved natural scene statistics model. *Digital Signal Processing*, 57, 56-65.
- Yang, Y., & Ming, J. (2016). Image quality assessment based on the space similarity decomposition model. *Signal Processing*, 120, 797-805.
- Fu, J., Wang, H., & Zuo, L. (2016). Blind image quality assessment for multiply distorted images via convolutional neural networks. In *Acoustics, Speech and Signal Processing (ICASSP), 2016 IEEE International Conference on* (pp. 1075-1079). IEEE.
- Vlachos, M. D., & Dermatas, E. S. (2012). Non-uniform illumination correction in infrared images based on a modified fuzzy c-means algorithm. *Journal of Biomedical Graphics and Computing*, 3(1), 6-19.
- Mustafa, W. A., & Yazid, H. (2016). Background Correction using Average Filtering and Gradient Based Thresholding. *Journal of Telecommunication, Electronic and Computer Engineering (JTEC)*, 8(5), 81-88.
- Mustafa, W. A., Yazid, H., & Yaacob, S. B. (2015). Illumination correction of retinal images using superimpose low pass and Gaussian filtering. In *Biomedical Engineering (ICoBE), 2015 2nd International Conference on* (pp. 1-4). IEEE.
- Sergyan, S. (2008). Color histogram features based image classification in content-based im-

- age retrieval systems. *2008 6th International Symposium on Applied Machine Intelligence and Informatics*, 221-224. doi:10.1109/SAMI.2008.4469170.
- Cano-García, A. E., Lazaro, J. L., Infante, A., Fernández, P., Pompa-Chacón, Y., & Espinoza, F. (2012). Using the standard deviation of a region of interest in an image to estimate camera to emitter distance. *Sensors (Basel)*, 12(5), 5687-5704. doi:10.3390/s120505687.
- Vallat-Evrard, L., Chagas, L., Passas, R., & Reverdy-Bruas, N. (2019). High dynamic range capture and sensor calibration to improve microscale halftone ink and paper surface quantification. *Review of Scientific Instruments*, 90(8), 083706. doi:10.1063/1.5099444.
- Smith, S. W. (1999). *The Scientist and Engineer's Guide to Digital Signal Processing Second Edition*. San Diego, California: California Technical Publishing.
- Teillet, P. M., Fedosejevs, G., Gauthier, R. P., O'Neill, N. T., Thome, K. J., Biggar, S. F., ... & Meygret, A. (2001). A Generalized Approach to the Vicarious Calibration of Multiple Earth Observation Sensors Using Hyperspectral Data. *Remote Sensing of Environment*, 77(3), 304-327. doi:10.1016/S0034-4257(01)00211-5.
- Syafrudin, A. H., Hadi, S., Salaswati, S., & Hasbi, W. (2018). Pre-flight radiometric model of linear imager on LAPAN-IPB satellite. *IOP Conference Series: Earth and Environmental Science*, 149(1). IOP Publishing.
- Erdogan, T. (2011). *Optical Filters, The Standard in Optical Filters for Biotech & Analytical*.

